MAGNETIC RESONANCE IN CHEMISTRY, VOL. 35, 845–853 (1997)

Assignment of Backbone NMR Resonances and Secondary Structural Elements of a Reduced Monomeric Mutant of Copper/Zinc Superoxide Dismutase

Lucia Banci, Marco Benedetto, Ivano Bertini,* Rebecca Del Conte, Mario Piccioli, Thierry Richert† and Maria Silvia Viezzoli
Department of Chemistry, University of Florence, Via Gino Capponi 7, I-50121 Florence, Italy

An extensive series of three-dimensional, triple resonance experiments were performed on a fully labeled ^{13}C, ^{15}N monomeric form of human copper/zinc superoxide dismutase which contains 153 amino acids. The present system, in addition to the mutations at the subunit–subunit interface (Phe50 → Glu, Gly51 → Glu) which lead to the monomeric form, carries the mutation of the Glu133 to Gln, a residue at the active channel entrance. Firm assignment was found for 97% of the protons, 99% of the $^{13}C\alpha$, 91% of the ^{15}N, 98% of $^{13}C(O)$ and 90% of the $^{13}C\beta$ backbone resonances. Analysis of the chemical shift values of $^{13}C\alpha$, $H\alpha$, $^{13}C\beta$ and ^{13}CO, of $^{3}J_{HNH\alpha}$ coupling constants, of NOEs between backbone protons and of the H–D exchange behavior of amide protons permits the unequivocal detection of elements of secondary structure. The secondary structure of the present monomeric form is very similar to that of the WT enzyme, although the enzymatic activity is 20% of that of the WT protein.
© 1997 John Wiley & Sons, Ltd.

Magn. Reson. Chem. **35**, 845–853 (1997) No. of Figures: 5 No. of Tables: 1 No. of References: 41

Keywords: NMR; ^{13}C NMR; ^{1}H NMR; copper/zinc superoxide dismutase; structure

Received 21 March 1997; revised 10 June 1997; accepted 21 June 1997

INTRODUCTION

Copper/zinc superoxide dismutase (SOD) is an enzyme which catalyzes the dismutation of the superoxide radical to hydrogen peroxide and dioxygen.[1–5] Copper ion is the catalytic center[6,7] and both oxidation states Cu^{2+} and Cu^{+} are significant for catalysis according to the following reactions:

$$Cu^{2+} + O_2^{-} \rightarrow Cu^{+} + O_2$$

$$Cu^{+} + O_2^{-} + 2H^{+} \rightarrow Cu^{2+} + H_2O_2$$

It is likely that superoxide binds or goes very close to the catalytic center, which is the copper ion, at the bottom of a 10 Å depth cavity.

The enzyme has, at physiological pH, an overall negative charge of −4. However, the side-chains of some residues in the active site channel form a positive electrostatic field within the catalytic cavity.[8] The electrostatic interaction of the substrate with the whole protein and inside the cavity are critical for determining the catalytic rates.[8–15]

Most of the known SOD isoenzymes are dimeric, consisting of two subunits interacting through a hydrophobic patch. Each subunit has 153 amino acids; therefore, monomeric forms are suitable for investigations through NMR for obtaining the solution structure. We succeeded in obtaining a soluble monomeric form of SOD by substituting the two hydrophobic residues Phe50 and Gly51 at the subunit–subunit interface with two negatively charged Glu residues (denoted as M2SOD species).[16] Such a mutant loses most of the enzymatic activity of the dimeric enzyme.[16] On the other hand, it has already been reported that, upon substitution of Glu133, located at the entrance of the cavity, with Gln, a 2–3-fold increase in activity is observed.[13,14]

We have produced the Gln133 variant of the monomeric Glu50–Glu51 SOD (Q133M2SOD),[17] which has higher activity with respect to the M2SOD form and whose reduced form is here characterized by ^{1}H, ^{13}C and ^{15}N NMR spectroscopy. The long-term goal of this research is the solution structure determination of the protein. In this way, many mutants can be studied and a firm assessment can be made about the relationship between solution structure and activity. In this paper we report the isolation of the double ^{13}C- and ^{15}N-labeled protein from a bacterial culture grown on minimal medium and a series of NMR experiments on the reduced form which have led to an extensive backbone assignment.

* *Correspondence to:* I. Bertini. *e-mail*: bertini@lrm.fi.cnr.it
† *Present address:* Bruker Spectrospin, rue de l'Industrie, Weissembourg, France.
Contract grant sponsor: CNR 'Comitato Scienze Chimiche'; *Contract grant number*: ERBFMGECT950033.
Contract grant sponsor: European Union; *Contract grant number*: CHRX-CT94-0540.

© 1997 John Wiley & Sons, Ltd. CCC 0749–1581/97/120845–09 $17.50

These results have allowed us to determine the elements of secondary structures of the monomeric form and to compare them with the analogous data obtained for the dimeric protein in the solid state through x-ray diffraction studies.[18]

EXPERIMENTAL

Sample preparation

The monomeric species of human SOD, where the Phe50 and Gly51 residues at the subunit–subunit interface have been replaced by two hydrophilic Glu residues (M2) and where a further mutation at position 133 (Glu to Gln) has been introduced (Q133M2SOD), has been expressed as already reported.[17] The *E. coli* TOPP1 strain (Stratagene) was transformed with the plasmid carrying the mutated SOD gene. The advantage of using this type of strain with respect to the MC1061, used in the past to express recombinant human SOD,[17] is that TOPP1 grows at a high level even on minimal medium and it is completely auxotrophic, allowing us to obtain complete and uniform labeling. The cells were grown in minimal medium (M9), containing 2 g l^{-1} [^{13}C]glucose and 6 g l^{-1} [^{15}N]ammonium sulfate. Protein purification was performed as already reported.[17] The resulting samples were fully enriched in ^{15}N and ^{13}C. Two 2.5 mM samples of labelled protein were prepared, one in H_2O and one in D_2O, both in 20 mM phosphate buffer (pH 5.1). The sample in D_2O was exchanged eight times against D_2O buffer by centrifugation. Reduction was achieved by addition of a 0.1 M solution of sodium isoascorbate (the final concentration of ascorbate was 5 mM) in phosphate buffer, under anaerobic conditions. The H_2O sample contained 10% of D_2O for the lock signal.

NMR spectroscopy

The NMR experiments were performed on a Bruker AMX 600 or DMX 600 spectrometer operating at 14.1 T and on a Bruker Avance 800 spectrometer operating at 18.8 T. All experiments were performed with a triple resonance 5 mm probe and with a BGU unit for self-shielded *z*-gradients. All NMR spectra were collected at 298 K. Proton chemical shifts are referenced to the H_2O signal at 4.81 ppm relative to sodium, 4,4-dimethyl-4 silapentane-1-sulfomate. Nitrogen chemical shifts are calibrated by assigning the $(^{15}NH_4)_2SO_4$ signal a shift of 21.6 ppm at 298 K. ^{13}C chemical shifts are referenced by assigning the dioxane signal in a 10% solution of dioxane in H_2O a shift of 69.46 ppm at 298 K.[19]

The following three-dimensional, triple resonance experiments were performed in H_2O solutions: HNCA,[20] HN(CO)CA,[21] HNCO,[22] (HCA)CO(CA)NH,[23] HN(CA)HA[24,25] and HN(COCA)HA.[26] The following experiments were also performed in H_2O solutions: HNHA,[27] NOESY-^{15}N HSQC[28] and ^{15}N HMQC-TOCSY.[29] To identify side-chain spin patterns, an (H)C(CO)NH-TOCSY[30] experiment was recorded in H_2O solution, together with (H)CCH-TOCSY[31] and H(C)CH-TOCSY[31] experiments in D_2O solutions.

All the experiments were performed using pulsed field gradients (PFGs) along the *z*-axis. For most of the experiments, PFGs were applied during INEPT and inverse-INEPT transfers, when the magnetization of interest is as $I_z S_z$ component. In this case PFGs will defocus all the other components of the magnetization and will improve water suppression.[31] Unless indicated otherwise, quadrature detection in the indirect dimensions was performed in the TPPI mode[32] and water presaturation was achieved through off-resonance DANTE irradiation.[33] ^{15}N HSQC experiments were also collected with the WATERGATE scheme and with a flip-back sequence.[34,35] No additional signals were observed with respect to the presaturated experiments. For the HNCA and HN(CO)CA experiments, the 3D experiments consisted of 512 (^{1}H) × 60 (^{15}N) × 180 (^{13}C) real points. Spectral windows of 4000 Hz (^{1}H) × 2049 Hz (^{15}N) × 3332 Hz (^{13}C) were used; 32 scans for each experiment were collected. HN(CA)HA and HN(COCA)HA were collected over 512 (^{1}H) × 104 (^{15}N) × 112 (^{1}H) real points. Spectral windows of 4000 Hz (^{1}H) × 2315 Hz (^{15}N) × 2404 Hz (^{1}H) were used. Two different HN(CA)HA experiments were performed, in order to optimize the identification of Gly residues. The HNCO experiment was performed with 512 (^{1}H) × 60 (^{15}N) × 180 (^{13}C) real data points over spectral windows of 4000 Hz (^{1}H) × 2049 Hz (^{15}N) × 1667 Hz (^{13}C). The (HCA)CO(CA)NH experiment was performed with 2048 (^{1}H) × 80 (^{15}N) × 88 (^{13}C) points. Spectral windows of 7788Hz (^{1}H) × 1712Hz (^{15}N) × 1786Hz (^{13}C) were used. For this experiment, water suppression was achieved through the WATERGATE sequence [34] and the experiments recorded in the States mode[36] for phase-sensitive detection in both indirect dimensions. A constant time evolution in the nitrogen dimension and a semi-constant time in the carbonyl dimension were used.

The HNHA experiment was performed with 768 real (^{1}H) × 64 complex (^{1}H) × 20 complex (^{15}N) data points. Spectral windows of 2315 Hz for ^{15}N and of 8000 Hz for both ^{1}H dimensions were used. The States mode[36] for phase-sensitive detection in both indirect dimensions was used. To extract the $^3J_{HNH\alpha}$ coupling constant, HNHA was also performed at 800 MHz with 2048 real (^{1}H) × 46 complex (^{15}N) × 56 complex (^{1}H) data points. States TPPI was used for both indirect dimensions. The final data matrix was 512 (^{1}H) × 128 (^{1}H) × 512 (^{15}N). ^{15}N HMQC-TOSCY was performed with 768 (^{1}H) × 64 (^{15}N) × 128 (^{1}H) points over spectral windows of 8064 Hz (^{1}H) × 2404 Hz (^{15}N) × 4000 Hz (^{1}H). NOESY-^{15}N HSQC, performed at 800 MHz, was recorded with 2048 (^{1}H) × 96 (^{15}N) × 340 (^{1}H) points; 3012 and 9615 Hz windows were used, respectively, for ^{15}N and both ^{1}H dimensions. The mixing time was 130 ms. (H)CCH-TOCSY and H(C)CH-TOCSY were performed using 512 (^{1}H) × 74 (^{13}C) × 174 (^{1}H) points. Spectral windows of 5000 Hz

© 1997 John Wiley & Sons, Ltd.

(^{1}H) × 9615 Hz (^{13}C) × 4000 Hz (^{1}H) were used. Both experiments were performed using PFGs for coherence selection and both experiments were acquired using the States and echo–antiecho mode for indirect dimensions. The (H)C(CO)NH experiment was performed with 2048 (^{1}H) × 64 (^{15}N) × 192 (^{13}C) data points over spectral windows of 10535 Hz (^{13}C) × 1712 Hz (^{15}N) × 7788 Hz (^{1}H).

Data were processed with the standard Bruker software packages (UXNMR, XWINNMR) or with the software package PROSA (ETH, Zurich).[37] Data analysis and assignment were performed using the program XEASY (ETH, Zurich).[38]

RESULTS AND DISCUSSION

Backbone assignment

The overall strategy for the assignment of the NMR resonances of the backbone nuclei in the Q133M2SOD was that of identifying, in the first stage, the amide groups in the ^{15}N HSQC spectra. Then, the five resonances of a given residue [HN(i), N(i), Cα(i), Hα(i) and CO(i)] were identified and the connectivities between subsequent amino acids were assigned. Assignments were confirmed by the analysis of 3D NOESY-^{15}N HSQC experiments. A ^{1}H–^{15}N HSQC spectrum is reported in Fig. 1; 139 cross peaks, which are identified as peptidic NH resonances, are observed out of the 147 expected signals from the non-proline residues.

Five 3D experiments were used to identify the HN, N, Cα, Hα resonances for each amino acid, i.e. HNCA, HN(CO)CA, HN(CA)HA, HN(COCA)HA and HNHA. The HNCA experiment correlates each HN group with both the intra- and the neighboring inter-residue Cα. These two types of connectivities are discriminated using the HN(CO)CA experiment, in which only the inter-residue HN–Cα coupling is observed.

The identification of Hα was then carried out on a similar basis. The HN(CA)HA experiment correlates each HN group with the intra- and the neighboring inter-residue Hα. The latter can be discriminated through both the HN(COCA)HA and the HNHA experiments. The HN(COCA)HA connects the HN group of each residue with the Hα of the previous residue, while the HNHA experiment mainly links each HN resonance with the intra-residue Hα.

To complete the backbone assignment, information from ^{13}CO resonances is also needed. Two 3D experiments, HNCO and (HCA)CO(CA)NH, were performed in order to identify the carbonyl resonances and to

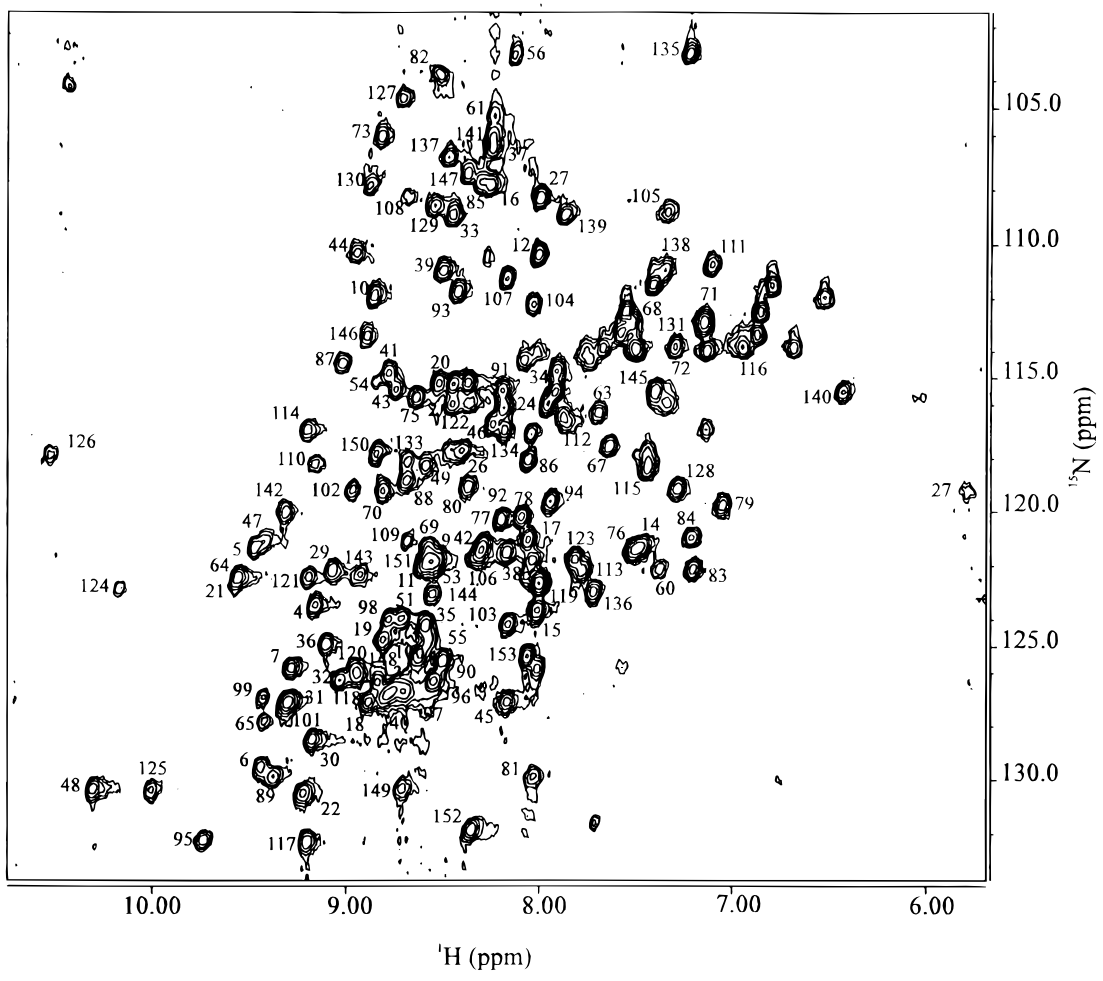

Figure 1. 600 MHz ^{1}H–^{15}N HSQC spectrum of reduced Q133M2SOD protein at 298 K and pH 5.1.

© 1997 John Wiley & Sons, Ltd.

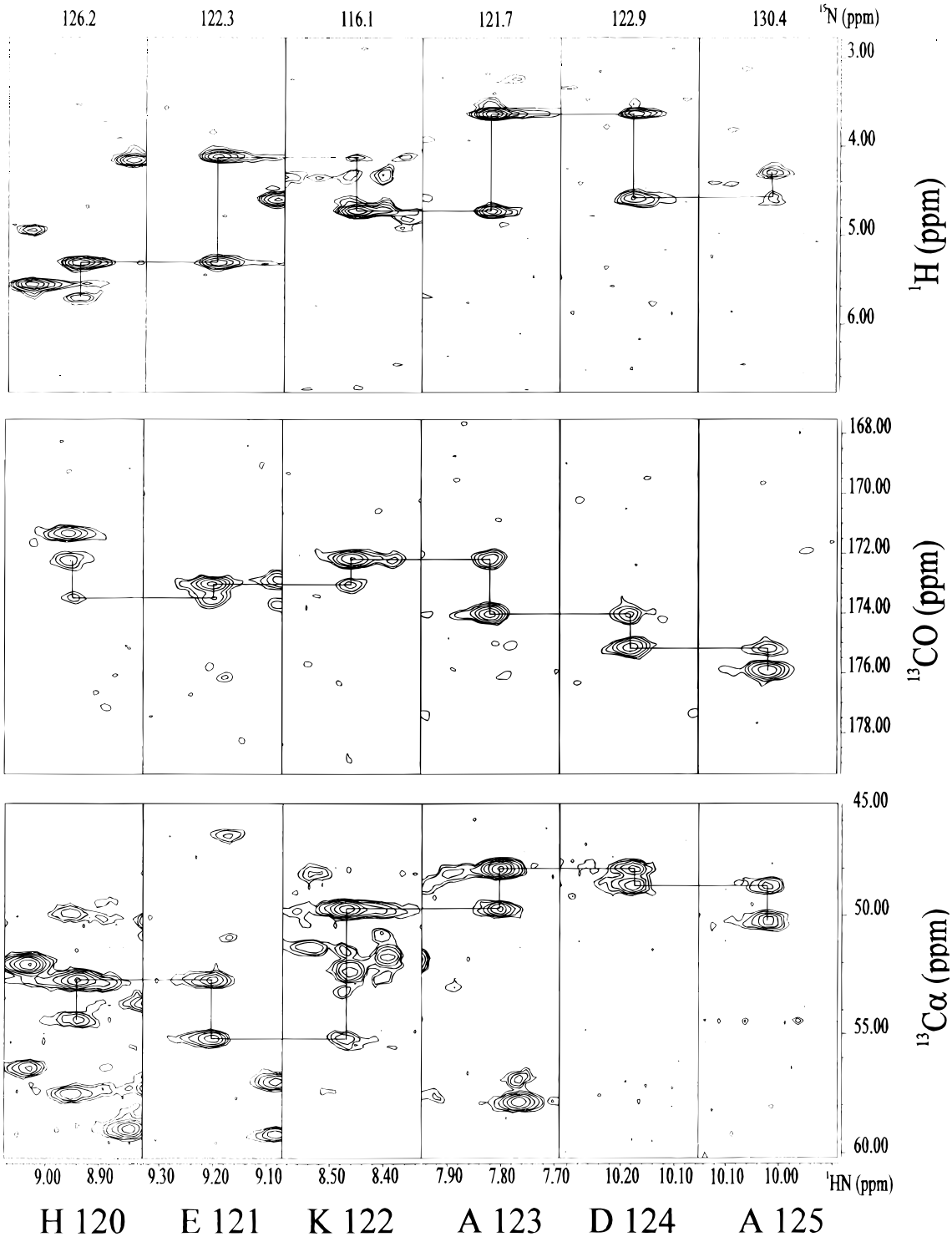

Figure 2. Example of the sequential connectivities among the $^{13}C\alpha$, $^{1}H\alpha$, and ^{13}CO resonances for the fragments 120–125 in reduced Q133M2SOD. F3–F1 slices are taken from an HN(CA)HA experiment (top), (HCA)CO(CA)NH (middle) and HNCA (bottom).

solve some ambiguities in the sequential connectivities. The (HCA)CO(CA)NH experiment correlates the amide resonances (HN and N) with the carbonyl resonance of a given residue and with that of the previous one, while the HNCO experiment provides the correlation only between the HN and ^{15}N resonances and that of ^{13}CO of the previous residue.

The sequential assignment was then perfomed using the inter-residue connectivities available for $^{13}C\alpha$, $H\alpha$ and ^{13}CO nuclei. While the assignment of the signals of a single type of resonances was sufficient to solve all the ambiguities in the assignment originating from overlap, the assignment of all these three nuclei for each residue allowed us to obtain an unambiguous assignment for the backbone resonances of 129 out of the 139 residues that were identified in the ^{15}N HSQC spectrum. As an

© 1997 John Wiley & Sons, Ltd.

example, Fig. 2 shows the sequential connectivities between the $^{13}C\alpha$, Hα and ^{13}CO resonances for the fragment 120–125.

With these experiments, however, assignment was not achieved for the residues 23–27 and 50–61. The assignment was then extended using the HC(CO)NH-TOCSY experiment, in which the coupling between each amide resonance with those of the aliphatic side-chain carbons of the previous residue is detected. Such an experiment allowed us to identify the residues 23–27, 50–56 and 59–61.

The HC(CO)NH-TOCSY experiment, together with H(C)CH-TOCSY and (H)CCH-TOCSY maps collected in D_2O solution, confirmed the assignment of all the backbone resonances already obtained and allowed the assignment of all side-chain proton and carbon resonances.

The residues for which the HN groups are not observed, which probably are the most mobile and solvent accessible, are Lys23, Ser25, Glu50, Asp52, Cys57, Thr58, Ser59 and Glu132, which are localized in well defined regions of the protein. Indeed, the region 21–26 is largely hydrophilic as it is constituted by two Glu, one Gln, one Asn, one Ser and one Lys. The hydrophilicity could account for the fast exchange with the solvent of some of the amide protons in this region. Similar considerations may hold for the region 49–52 (three consecutive Glu and one Asp).

As far as the two residues 57–58 are concerned, we should recall that Cys57 is involved in a disulfide bridge with Cys146, in the dimeric protein. The large downfield shift of $^{13}C\beta$ of Cys146 is a clear indication that Cys146 is in the oxidized form. Furthermore, it has shown that isomerization of a disulfide bridge may lead to line broadening of the signals due to the atoms affected by this equilibrium. The lack of observation of the Cys57 and Thr58 signals may originate from the possible presence of this conformational equilibrium. The three-dimensional solution structure of this mutant, which is now in progress, will allow us to verify such hypothesis.

Secondary structure elements

The elements of secondary structure were determined on the basis of the chemical shift index (CSI), as originally proposed by Wishart and Sykes[19] and on the basis of the backbone NOEs that have been assigned in a 3D NOESY-^{15}N HSQC experiment. $^3J_{HNH\alpha}$ coupling constants were extracted from analysis of peak intensity in a HNHA experiment, according to Vuister and Bax.[27] To compensate for the expected decrease in J values due to differential relaxation behavior of in-phase and anti-phase magnetization during the experiment, the observed J values were multiplied by a factor of 1.17. Such a factor was empirically estimated from the molecular mass of the present protein. The analysis of CSI for $^1H\alpha$, $^{13}C\alpha$, ^{13}CO and $^{13}C\beta$ is reported in Fig. 3, together with amide hydrogen–deuterium exchange and $^3J_{HNH\alpha}$. The ternary index +, 0, − was used for defining the CSI, where + and − indicate downfield and upfield shifts, respectively, with respect to random coil chemical shift values (0). It is expected that residues in β-strands show positive (downfield) deviations for the ^1H and $^{13}C\beta$ resonances while negative deviations are observed for the $^{13}C\alpha$ and ^{13}CO resonances. The opposite is expected for residues in α-helices. A secondary structural element is considered to be present when it is consistent with three out of the four different sets of chemical shift data (or two out of three if the $^{13}C\beta$ shift is not present or not available).

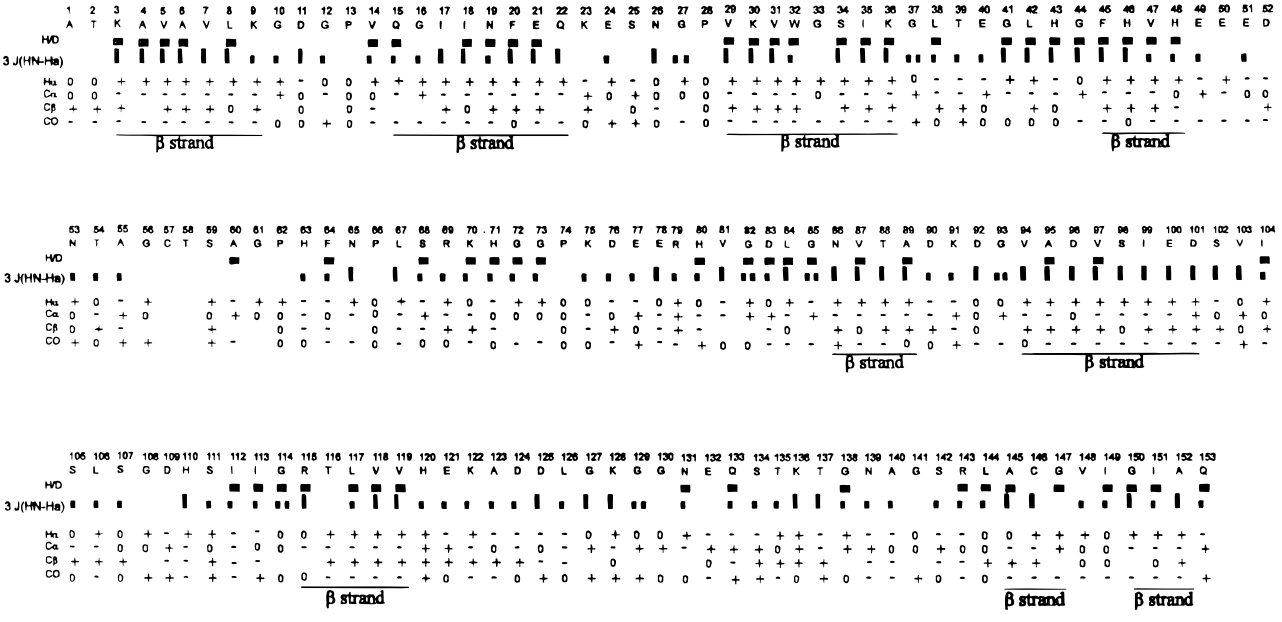

Figure 3. Summary of chemical shift index on the backbone resonances for reduced Q133M2SOD. They are relevant to define the secondary structure. The+ and − indicate that the chemical shift value is downfield or upfield with respect to what is expected for a random coil structure (0). Reference values and tolerances are taken from Refs 19, 40 and 41. Black bars below the CSI indicate the consensus sequence observed on this basis. Amide hydrogen–deuterium exchange rates are also reported. Black squares indicate HN signals that were observed in an HSQC spectrum of a sample 2 months after it had been dissolved in D_2O. $^3J_{HNH\alpha}$, obtained from a 3D HNHA experiment, are reported. Large bars indicate ^3J values >8 Hz and small bars indicate ^3J values <8 Hz.

© 1997 John Wiley & Sons, Ltd.

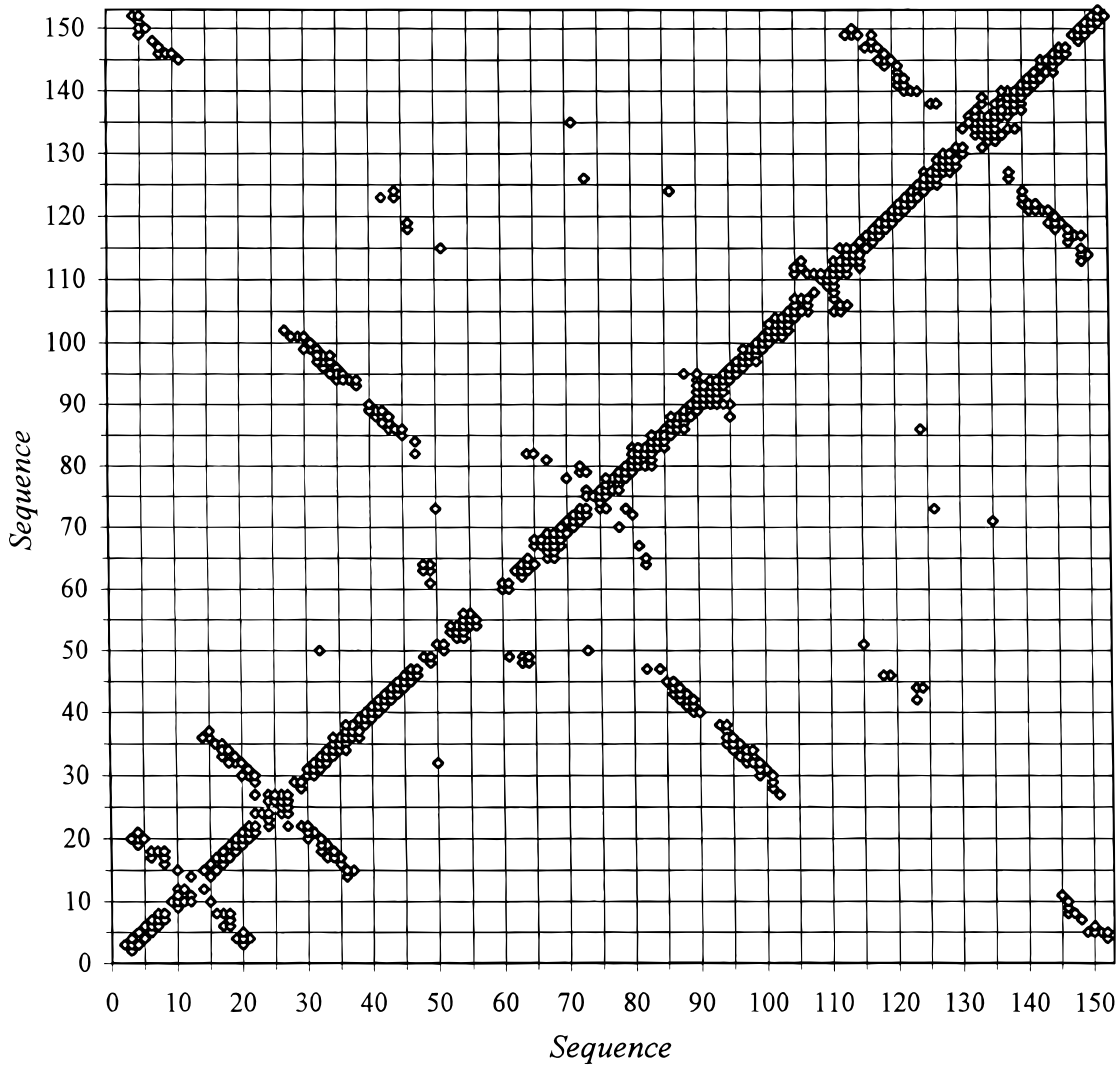

Figure 4. Backbone proton NOEs for Q133M2SOD. Reported NOEs arise from HN–HN or HN–Hα interactions. They were assigned in a ^{15}N NOESY-HSQC experiment, collected at 800 MHz, 298 K, pH 5.1.

On the basis of CSI, β-strands were found in the regions 3–9, 15–22, 29–36, 45–47, 86–89, 94–101, 115–119, 145–147 and 150–152. No indication of α-helices was observed from this parameter. The measured $^3J_{HNH\alpha}$ values were in satisfactory agreement with conclusions drawn observed from CSI. The average values observed for those regions in which extended secondary structure elements are present are consistent with what is expected for anti-parallel β-sheets.[39] The interactions among different β-strands can be determined from the data shown in Fig. 4, which reports the NOEs between HN signals with HN or Hα of any other residue. A total of 689 backbone NOEs were detected, of which 292 arise from sequential connectivities, 264 from long- and medium-range connectivities and 133 are intra-residue NOEs. Each of the observed strands is connected with two other strands in an anti-parallel β-sheet motif, as can be observed by the anti-diagonal bands in Fig. 4. The two small β-strands 145–147 and 150–152 are separated by only two residues and their pattern of NOE (Fig. 4) is consistent with a single β-strand involving residues 145–152, with the stretch 145–152 being anti-parallel to 3–9 residues. The resulting topology is consistent with a Greek key, eight-stranded β-barrel and is shown in Fig. 5.

The observed β-strands can be compared with those observed in the native, dimeric human protein.[18] All the β-strands observed in the x-ray structure of the dimeric protein are found also in the present monomeric form. The strand encompassing two copper-binding histidines, which involves residues 41–48 in the native dimeric protein, is also present for the same residue stretch in the present monomeric form on the basis of backbone NOEs. Although the CSI parameter indicates a shortening to 45–47 in the present derivative, the $^3J_{HNH\alpha}$ values account for a β-sheet motif in the fragment 41–45, with coupling constants being invariably larger than 8 Hz. Also the terminal strand (146–152 in the native dimeric protein) is found equal in the present monomeric form to that observed in the dimeric protein on the basis of backbone NOEs even if, as mentioned earlier, residues 148–149 do not match the criteria dictated by Wishart and Sykes.[19] Also, the $^3J_{HNH\alpha}$ values for residues 148–149 are <8 Hz. It is therefore reasonable to propose that a β-strand is spanning 145–152, consistent with backbone NOEs, but it is likely that

© 1997 John Wiley & Sons, Ltd.

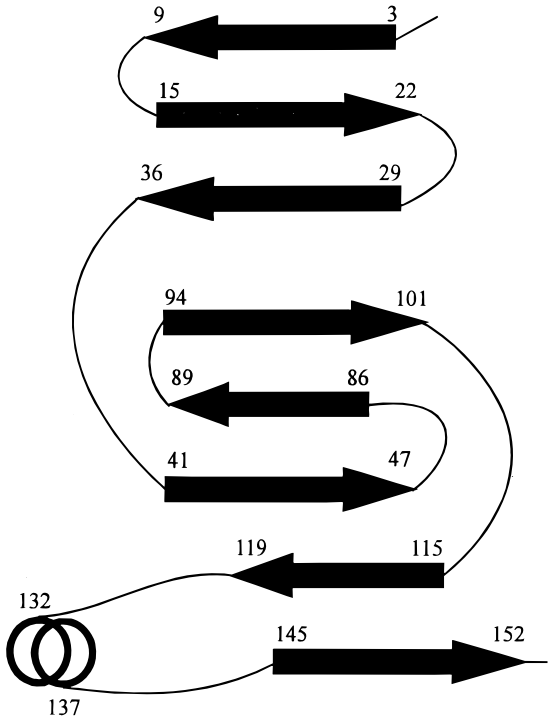

Figure 5. Schematic representation of the secondary structure elements of Q133M2SOD. They were determined with either CSI or backbone NOEs.

some distortions from the extended configuration occur at residues 148–149.

A further comment, as far as secondary structure is concerned, is needed for the region 132–137, which is part of the electrostatic loop VII. In the native dimeric protein such a region forms a well defined, six-residue α-helix.[7,18] This protein region has been claimed to be important to promote recognition of the superoxide anion substrate. As already mentioned, the CSI index does not show evidence of an α-helix, as only Cα atoms are consistent with a helical structure. On the other hand, Hα(i)–HN($i + 3$) and Hα(i)–HN($i + 4$) NOEs have been found for Hαs of fragments 132–134 to the NHs of residues 135–138. These NOEs therefore indicate the presence of an α-helical structure for this protein part.

Overall, there is clear evidence that the β-barrel structure of eight anti-parallel β-strands, which characterizes the secondary structure of SOD, is unaltered in the present monomeric form with respect to what is observed in the native dimeric protein.

The H–D exchange behavior was also been analyzed through a ^{15}N HMQC experiment recorded in D_2O solution, as reported in Fig. 3. Most of the amide protons of the protein regions belonging to β-sheets do not exchange with the bulk solvent as they are involved in extensive H-bond networks. However, there are some regions, characterized by the presence of non-exchanging NH protons, that are not part of β-sheets. This is the case with fragments 70–73 and 80–85. His71 and His80 are residues directly coordinated to the Zn(II) ion. The latter, in the native dimeric protein, is buried inside the protein. These residues are less accessible to the solvent, thus preventing the NHs from

Table 1. Backbone ^{1}H, ^{13}C and ^{15}N resonance assignments for the reduced monomeric species Q133M2SOD at 298 K and pH 5.1

residue	HN	N	Cα	Hα	CO	Cβ
A-1	—	—	52.3	4.25	174.0	20.3
T-2	8.55	116.5	62.5	4.45	172.4	70.1
K-3	8.73	126.3	55.0	5.38	174.5	36.3
A-4	9.18	123.5	50.8	5.32	175.3	23.7
V-5	9.49	121.3	60.4	5.35	173.1	36.2
A-6	9.45	129.6	51.0	4.89	174.5	23.2
V-7	9.30	125.9	62.0	4.34	175.7	31.7
L-8	8.78	126.7	54.3	4.30	176.1	42.7
K-9	8.52	121.9	55.3	4.90	175.2	35.6
G-10	8.86	112.0	46.0	4.28/4.85	173.3	—
D-11	8.62	121.9	54.17	4.69	176.5	40.5
G-12	8.01	110.7	44.4	3.92/4.28	173.6	—
P-13	—	—	63.6	4.51	176.7	32.6
V-14	7.47	121.3	63.0	4.51	176.0	30.3
Q-15	8.02	123.7	54.0	4.87	174.3	—
G-16	8.27	107.9	46.9	3.97/4.56	171.0	—
I-17	8.07	121.0	61.3	4.73	174.1	40.7
I-18	8.87	127.1	56.9	4.22	172.5	37.6
N-19	8.81	125.1	52.5	4.82	172.3	40.2
F-20	8.52	115.5	55.5	5.80	176.3	43.2
E-21	9.57	122.5	56.0	5.39	173.7	34.2
Q-22	9.23	129.9	54.5	4.96	174.6	—
K-23	—	—	59.9	4.07	176.2	33.4
E-24	8.20	116.3	54.3	4.66	177.2	—
S-25	—	—	61.0	3.98	174.7	62.5
N-26	8.40	117.8	53.2	4.68	175.0	38.0
G-27	8.00	108.3	44.8	4.02/4.58	172.1	—
P-28	—	—	63.1	4.58	176.2	32.4
V-29	9.09	122.0	61.3	4.60	175.4	33.3
K-30	9.19	128.5	55.9	4.99	175.3	34.2
V-31	9.30	127.3	60.5	4.94	175.5	33.4
W-32	9.04	126.4	56.2	5.60	173.4	32.1
G-33	8.46	109.0	44.8	3.90/4.99	171.5	—
S-34	7.91	114.7	57.0	5.56	173.0	65.2
I-35	8.58	124.1	60.3	4.59	173.0	41.1
K-36	9.11	125.1	54.6	5.33	175.5	35.1
G-37	8.25	106.7	45.6	3.84/4.04	174.9	—
L-38	8.17	121.6	53.5	3.98	177.0	44.3
T-39	8.50	111.1	61.2	4.20	176.1	69.5
E-40	8.81	126.8	57.7	3.69	176.2	30.2
G-41	8.79	114.7	43.3	3.78/4.68	173.2	—
L-42	8.30	121.1	55.8	4.81	177.4	44.2
H-43	8.76	115.7	54.3	4.33	164.7	31.6
G-44	8.96	110.5	47.4	3.21/4.72	171.8	—
F-45	8.17	127.1	56.0	5.61	172.3	42.6
H-46	8.25	116.8	52.3	5.65	175.2	36.4
V-47	9.41	121.1	62.2	4.62	176.8	32.4
H-48	10.34	130.3	56.2	5.00	174.8	30.6
E-49	8.59	118.4	60.1	3.83	174.8	—
E-50	—	—	55.4	4.49	175.5	30.8
E-51	8.71	123.8	56.4	3.82	174.5	—
D-52	—	—	54.2	4.59	174.5	41.9
N-53	8.54	121.9	53.0	4.90	176.4	39.4
T-54	8.82	115.5	62.2	4.32	175.7	71.0
A-55	8.58	124.3	53.8	4.15	178.1	18.4
G-56	8.13	103.4	45.3	4.22/4.34	175.0	—
C-57	—	—	—	—	—	—
T-58	—	—	—	—	—	—
S-59	—	—	58.50	4.66	174.4	63.8
A-60	7.40	122.0	54.2	4.00	176.6	—
G-61	8.23	105.3	44.8	4.01/4.33	—	—
P-62	—	—	62.3	4.76	175.5	32.2
H-63	7.71	116.3	54.8	3.95	175.0	30.6
F-64	9.58	122.6	57.8	4.52	175.3	38.7

© 1997 John Wiley & Sons, Ltd.

Table 1—*Continued*

residue	HN	N	Cα	Hα	CO	Cβ
N-65	9.42	127.9	51.2	5.17	172.9	—
P-66	—	—	64.5	4.34	177.1	30.7
L-67	7.64	117.6	54.2	4.46	175.8	40.5
S-68	7.50	113.1	59.2	3.92	174.0	60.4
R-69	8.58	121.1	53.9	4.63	176.6	32.7
K-70	8.82	119.3	56.0	4.45	173.1	33.4
H-71	7.14	113.1	56.0	2.88	174.5	31.4
G-72	7.29	114.0	44.7	4.01/4.61	171.8	—
G-73	8.83	106.3	44.6	3.75/4.40	172.7	—
P-74	—	—	63.8	4.46	178.8	31.0
K-75	8.65	116.0	55.0	4.38	176.8	31.3
D-76	7.52	121.5	54.6	4.52	175.8	41.9
E-77	8.30	121.4	58.7	3.95	177.2	29.7
E-78	8.10	120.3	55.3	4.15	171.5	27.8
R-79	7.04	119.8	54.6	4.67	175.4	32.1
H-80	8.38	119.2	53.8	4.56	179.0	29.0
V-81	8.10	129.9	61.4	3.50	176.7	—
G-82	8.53	98.6	46.2	4.12/4.48	173.5	—
D-83	7.19	122.2	55.9	4.90	172.2	39.4
L-84	7.21	121.1	53.8	4.65	176.5	41.7
G-85	8.31	108.3	46.6	3.65/3.99	170.9	—
N-86	8.07	118.2	52.3	5.81	177.2	44.2
V-87	9.03	114.8	59.1	4.57	174.7	32.0
T-88	8.70	118.9	62.0	4.63	173.5	69.6
A-89	9.38	129.9	49.7	4.62	177.5	20.9
D-90	8.50	125.5	52.8	4.54	177.1	41.6
K-91	8.20	115.5	58.5	3.94	177.4	31.6
D-92	8.20	120.3	54.3	4.76	176.3	41.2
G-93	8.43	112.0	47.3	3.93/4.17	172.9	—
V-94	7.94	119.5	61.5	4.69	176.6	32.6
A-95	9.75	132.2	50.2	5.15	174.9	20.2
D-96	8.56	126.3	54.3	5.00	175.8	41.2
V-97	8.71	126.8	62.2	4.07	176.5	32.9
S-98	8.80	123.5	58.0	5.17	173.1	62.3
I-99	9.44	126.9	60.2	4.69	174.3	44.2
E-100	8.63	125.2	55.5	5.42	175.4	32.4
D-101	9.31	127.5	54.7	5.13	174.5	47.1
S-102	8.98	119.3	58.4	4.82	172.8	63.8
V-103	8.17	124.2	64.1	4.06	178.4	32.0
I-104	8.08	112.5	62.9	4.14	172.7	39.8
S-105	7.32	109.0	55.8	4.52	173.2	65.3
L-106	8.32	122.0	54.0	4.58	174.9	40.1
S-107	8.16	111.5	57.8	4.64	173.8	65.4
G-108	8.68	107.9	45.1	4.04/4.63	175.8	—
D-109	8.70	121.1	57.0	4.34	178.1	40.0
H-110	9.16	118.4	53.2	5.00	173.1	28.4
S-111	7.11	111.0	57.7	3.94	177.0	64.1
I-112	7.85	116.7	60.8	3.79	174.9	36.6
I-113	7.77	122.2	61.8	3.25	177.5	34.5
G-114	9.21	117.1	45.4	3.47/4.20	173.2	—
R-115	7.43	118.4	53.8	4.31	174.5	—
T-116	6.98	113.7	63.3	4.72	173.1	70.5
L-117	9.23	132.3	54.0	4.80	174.7	44.1
V-118	8.95	125.9	61.6	4.68	173.8	35.8
V-119	8.04	121.9	58.4	5.71	174.6	35.4
H-120	8.93	126.0	56.9	5.33	176.0	33.4
E-121	9.19	122.4	59.2	4.12	175.5	32.5
K-122	8.43	116.1	53.9	4.72	174.7	34.8
A-123	7.82	121.9	52.2	3.64	176.5	19.9
D-124	10.19	122.9	52.9	4.58	177.6	42.9
D-125	10.02	130.4	54.3	4.30	178.4	39.3
L-126	10.53	117.9	55.0	3.44	177.0	38.0
G-127	8.73	104.8	45.9	3.47/4.20	177.1	—
K-128	7.28	119.2	54.5	4.56	177.5	31.7
G-129	8.54	108.8	46.1	3.75/4.06	175.3	—
G-130	8.88	108.1	46.2	3.76/4.00	173.5	—
N-131	7.14	113.1	50.7	4.91	175.5	—
E-132	—	—	59.3	4.06	174.8	29.1
Q-133	8.70	118.4	58.4	4.01	179.3	28.1
S-134	8.19	116.8	62.4	3.85	176.4	63.6
T-135	7.23	103.2	63.1	4.63	174.2	69.2
K-136	7.70	123.0	62.8	4.69	176.7	35.4
T-137	8.48	107.1	60.5	3.62	176.0	71.6
G-138	7.36	111.5	46.2	4.14/4.42	173.3	—
N-139	7.86	109.0	55.4	4.02	174.0	36.8
A-140	6.39	115.8	53.2	4.16	176.5	17.6
G-141	8.25	105.8	45.6	3.90/4.20	176.7	—
S-142	9.30	120.5	59.8	4.38	173.5	63.6
R-143	8.93	122.6	55.9	3.73	174.9	29.3
L-144	8.56	123.2	56.0	4.27	177.1	43.3
A-145	7.40	115.6	51.6	4.42	174.8	21.2
C-146	8.89	113.7	54.3	6.05	173.8	46.2
G-147	8.38	107.3	46.6	4.01/4.18	171.7	—
V-148	8.85	126.3	63.0	4.27	176.4	32.0
I-149	8.72	130.3	62.2	3.96	175.5	37.3
G-150	8.85	117.9	43.8	3.84/4.82	172.7	—
I-151	8.59	121.9	61.5	4.18	175.5	38.1
A-152	8.37	131.8	51.3	4.61	175.4	20.5
Q-153	8.06	125.4	57.3	4.16	180.8	—

exchanging. Most of the HN protons of fragment 94–101, one of the eight β-strands, disappear in D_2O solutions.

CONCLUSION

A series of NMR experiments on the fully ^{13}C- and ^{15}N-labeled monomeric copper/zinc superoxide dismutase Q133M2SOD were performed which has led to extensive assignments for the backbone nuclei and Cβ. Analysis of the backbone NOEs, of the observed CSI and of the $^{3}J_{HNH\alpha}$ couplings provided the elements of the secondary structure of the present monomeric SOD, including the eight β-sheets which form the β-barrel, and a short α-helix observed only because of backbone NOEs. The secondary structure is similar to that of the dimeric enzyme.

This is unambiguous proof that the large decrease in the activity, observed for all the investigated monomeric derivatives (about 5–10% of the corresponding mutant in the dimeric form), does not depend on changes in the β-barrel scaffold of the protein. On the other hand, we have already shown that changes in the copper chromophore do not account for the decrease in the activity.[16] This underlines the relevance of the tertiary structure. It is likely that structural variations and/or fluctuations occurring in the loops that define the active cavity of the enzyme are the factors controlling the catalysis.

Acknowledgements

The SON NMR LSF Utrecht, directed by Professor R. Kaptein, and the Frankfurt LSF, directed by Professor H. Rüterjans, are acknowledged for allowing us to perform some heteronuclear experiments.

© 1997 John Wiley & Sons, Ltd.

We are, in particular, grateful to Frank Lohr (University of Frankfurt) for his help and discussions. The contribution of Dr Roberta Pierattelli (University of Florence) in the early stage of this project is gratefully acknowledged. Thanks are also expressed to Dr Matteo Mariani (University of Groeningen) for the interpretation of the spectra. Chiron Corporation is acknowledged for having allowed us to use the expression vector pPHSODLaqI^q from which the plasmid encoding the present analog was obtained. Thanks are expressed to Dr Lindsay Eltis (University of Lavalle) for valuable suggestions and assistance in the preparation of the labeled sample. This work was financially supported by CNR 'Comitato Scienze Chimiche' and was carried out under the TMR Large Scale Facility Program (PARABIO, ERBFMGECT950033). T. R. acknowledges European Union for a post-doctoral fellowship (CHRX-CT94-0540).

REFERENCES

1. I. Fridovich, *Adv. Enzymol.* **41**, 35 (1974).
2. I. Fridovich, *Adv. Enzymol. Relat. Areas Mol. Biol.* **58**, 61 (1986).
3. J. S. Valentine and M. W. Pantoliano, in *Copper Proteins*, edited by T. G. Spiro, p. 291. Wiley, New York (1981).
4. B. Halliwell and J. M. Gutteridge, *Free Radicals in Biology and Medicine*, p. 22. Clarendon Press, Oxford (1989).
5. I. Bertini, S. Mangani and M. S. Viezzoli, *Adv. Inorg. Chem.* in press.
6. J. M. McCord and I. Fridovich, *J. Biol. Chem.* **244**, 6049 (1969).
7. J. A. Tainer, E. D. Getzoff, K. M. Beem, J. S. Richardson and D. C. Richardson, *J. Mol. Biol.* **160**, 181 (1982).
8. I. Klapper, R. Hagstrom, R. Fine, K. Sharp and B. Honig, *Proteins: Struct. Funct. Genet.* **1**, 47 (1986).
9. W. H. Koppenol, in *Oxygen and Oxoradicals in Chemistry and Biology*, edited by M. A. J. Rodgers and E. L. Powers, p. 671. Academic Press, New York (1981).
10. K. Sharp, R. Fine and B. Honig, *Science* **236**, 1460 (1987).
11. J. J. Sines, S. A. Allison and J. A. McCammon, *Biochemistry* **29**, 9403 (1990).
12. L. Banci, I. Bertini, C. Luchinat and R. A. Hallewell, *J Am. Chem. Soc.* **110**, 3629 (1988).
13. E. D. Getzoff, D. E. Cabelli, C. L. Fisher, H. E. Parge, M. S. Viezzoli, L. Banci and R. A. Hallewell, *Nature* (*London*) **358**, 347 (1992).
14. L. Banci, D. E. Cabelli, E. D. Getzoff, R. A. Hallewell and M. S. Viezzoli, *J. Inorg. Biochem.* **50**, 89 (1993).
15. B. A. Luty, S. El Amrani and J. A. McCammon, *J. Am. Chem. Soc.* **115**, 11874 (1993).
16. I. Bertini, M. Piccioli, M. S. Viezzoli, C. Y. Chiu and G. T. Mullenbach, *Eur. J. Biophys.* **23**, 167 (1994).
17. L. Banci, I. Bertini, C. Y. Chiu, G. T. Mullenbach and M. S. Viezzoli, *Eur. J. Biochem.* **234**, 855 (1995).
18. H. E. Parge, R. A. Hallewell and J. Tainer, *Proc. Natl. Acad. Sci. USA.* **89**, 6109 (1992).
19. D. S. Wishart and B. D. Sykes, *J. Biomol. NMR* **4**, 171 (1994).
20. L. E. Kay, M. Ikura, R. Tschudin and A. Bax, *J. Magn. Reson.* **89**, 496 (1990).
21. A. Bax and M. Ikura, *J. Biomol. NMR* **1**, 99 (1991).
22. A. L. Davis, R. Boelens and R. Kaptein, *J. Biomol. NMR* **2**, 395 (1992).
23. F. Löhr and H. Rüterjans, *J. Biomol. NMR* **6**, 189 (1995).
24. R. T. Clubb, V. Thanabal and G. Wagner, *J. Biomol. NMR* **2**, 203 (1992).
25. S. Seip, J. Balbach and H. Kessler, *J. Magn. Reson.* **100**, 406 (1992).
26. R. T. Clubb and G. Wagner, *J. Biomol. NMR* **2**, 389 (1992).
27. G. W. Vuister and A. Bax, *J. Am. Chem. Soc.* **115**, 7772 (1993).
28. G. Wider, D. Neri, G. Otting, and K. Wüthrich, *J. Magn. Reson.* **85**, 426 (1989).
29. D. Marion, L. E. Kay, S. W. Sparks, D. A. Torchia and A. Bax, *J. Am. Chem. Soc.* **111**, 1515 (1989).
30. T. M. Logan, E. T. Olejniczak, R. X. Xu, and S. W. Fesik, *J. Biomol. NMR* **3**, 225 (1993).
31. L. E. Kay, G. Xu, A. U. Singer, D. R. Muhandiram and J. D. Forman-Kay, *J. Magn. Reson. B* **101**, 333 (1993).
32. D. Marion and K. Wüthrich, *Biochem. Biophys. Res. Commun.* **113**, 967 (1983).
33. L. E. Kay, D. Marion and A. Bax, *J. Magn. Reson.* **84**, 72 (1989).
34. M. Piotto, V. Saudek and V. Sklenar, *J. Biomol. NMR.* **2**, 661 (1992).
35. S. Grzesiek and A. Bax, *J. Am. Chem. Soc.* **115**, 12593 (1993).
36. D. J. States, R. A. Habenkorn and D. J. Ruben, *J. Magn. Reson.* **48**, 286 (1982).
37. P. Güntert, V. Dotsch, G. Wider and K. Wüthrich, *J. Biomol. NMR* **2**, 619 (1992).
38. C. Eccles, P. Güntert, M. Billeter and K. Wüthrich, *J. Biomol. NMR* **1**, 111 (1991).
39. K. Wüthrich, *NMR of Proteins and Nucleic Acids*. Wiley, New York (1986).
40. D. S. Wishart, B. D. Sykes and F. M. Richards, *Biochemistry* **31**, 1647 (1992).
41. D. S. Wishart, C. G. Bigam, A. Holm, R. S. Hodges and B. D. Sykes, *J. Biomol. NMR* **5**, 67 (1995).

© 1997 John Wiley & Sons, Ltd.